International Seminar on Mineral Processing Technology (MPT-2008), April 22-24, 2008
Jointly Organized by Indian Institute of Mineral Engineers & National Institute for Interdisciplinary Science & Technology, CSIR, Trivandrum.

ADSORPTION MECHANISM OF LONG-CHAIN ALKYLAMINES ON QUARTZ AND ALBITE

A. Vidyadhar[1*], A. Das[2] and K. Hanumantha Rao[3]

[1,2]Mineral Processing Division, National Metallurgical Laboratory, Jamshedpur-831 007, India
[3]Division of Mineral Processing, Luleå University of Technology, SE-97187 LULEÅ, Sweden
[*]E-mail: ari@nmlindia.org

ABSTRACT

The mechanism of adsorption of long-chain alkylamines at pH 6-7 onto quartz and albite using the direct methods of FTIR and XPS spectroscopy. The spectroscopic data were correlated with the data of indirect methods of zeta-potential measurements and Hallimond flotation results. It was shown from infrared spectra that the amine cation forms strong hydrogen bonds with surface silanol groups. The XPS spectra revealed the presence of molecular amine together with the protonated amine on silicate surface. Based on these observations, a model of successive two-dimensional and three-dimensional precipitation was suggested to explain amine adsorption on silicate surface.

1. INTRODUCTION

The understanding of the mechanism of adsorption of long-chain alkyl amines and elucidation of the properties of the adsorbed layers is important for a variety of industrial applications. In particular, primary long-chain alkylammonium salts are most commonly used flotation collectors for beneficiation of silicates[1], principally because of their relatively high solubility. This problem was studied extensively by indirect methods of the measurement of contact angle, zeta-potential, surface forces and flotation recovery response during the last 60 years [2-4]. Untill recently, the adsorption of amines on silicates at neutral pH has been explained mainly by the Gaudin-Fuerstenau-Somasundaran model [5-7].

The objective of the present investigation is to study the adsorption of long-chain alkylamines at natural pH on quartz and albite by using direct spectroscopic methods of FTIR and XPS. It is intended to compare the spectroscopic data to flotation and zeta-potential results so as to distinguish the spectral characteristics for qualitative assessment of the adsorbed layer for surface hydrophobicity or hydrophilicity.

2. EXPERIMENTAL

2.1. Materials

The pure crystalline quartz and albite mineral samples obtained from Mevior S.A., Greece were used in the present investigations. The chemical analysis showed that quartz was about 99% pure with traces of aluminium (Al_2O_3, 0.1 wt%), calcium (CaO, 0.09 wt%) and iron impurities (Fe_2O_3, 0.046 wt%) and albite more than 98.5% purity with oxides content of 67.9 wt% SiO_2, 19.2 wt% Al_2O_3 and 11.7 wt%

Na_2O. The samples were crushed and ground in an agate mortar. The products were wet-sieved to obtain particle size fractions of –150+38 μm and –38 μm. A portion of –38 μm was further ground and micro-sieved in an ultrasonic bath to obtain –5 μm size fraction. The coarser size fraction, –150+38 μm, was employed for Hallimond flotation tests while the fines (–5 μm) were used in zeta-potential and FTIR investigations. The BET specific surface areas for albite coarser and fine fractions were determined to be 0.15 and 2.78 $m^2 g^{-1}$ and the respective specific surface areas for quartz size fractions were found to be 0.09 and 1.30 $m^2 g^{-1}$.

2.2. Reagents

The primary alkyl amines with 99% purity containing C_8, C_{12} and C_{16} chain-lengths were kindly supplied by the Akzo Nobel AB, Sweden. The acetate salts of C_{12} and C_{16} amines were prepared in benzene solvent by mixing equimolar amounts of the respective amine and acetic acid. The acetate salt crystallizes below the freezing temperature and it was purified thrice by recrystallization using fresh benzene each time. Analar grade NaOH and HCl were used for pH adjustment and deionized water was used in all the experiments.

2.3. Flotation Tests

The single mineral flotation tests were made using Hallimond cell of 100 ml volume. Exactly 1.0 g mineral sample was conditioned first in predetermined concentration of amine solution for 5 min and the suspension was transferred to the flotation cell. The flotation was conducted for 1 min at an air-flow rate of 8 ml min^{-1}. All the tests were performed at a neutral pH region of 6–7.

2.4. Zeta-potential Measurements

Zeta-potentials were determined using a Laser Zee Meter (Pen Kem Inc., model 501) equipped with video system employing a flat rectangular cell. 1.0 g l^{-1} mineral suspension was prepared in 10^{-3} KNO_3 supporting electrolyte solutions, conditioned for 1 hour at room temperature (22°C) in the presence of predetermined concentration of reagents and pH. The pH of the suspension at the time of measurement was reported in the results. After the measurements, the suspension was filtered through millipore filter paper (pore size 0.22 μm) and the solids are air-dried before recording the DRIFT infrared spectrum.

2.5. Diffuse Reflectance FT-IR Measurements

The infrared spectra were registered for all the samples after zeta-potential measurements on the air-dried –5 μm powder. The FTIR spectra were obtained with a Perkin-Elmer 2000 spectrometer with its own diffuse reflectance attachment. Typical spectrum was an average of 200 scans at 4 cm^{-1} resolution with a narrow band liquid nitrogen cooled MCT detector. Since the intensity of the bands with respect to adsorbed layers was low, the samples were not mixed with KBr. The untreated mineral powder was used as reference and the absorbance units were defined by the decimal logarithm of the ratio of initial mineral reflectance to the sample one. The atmospheric water was always subtracted. The area under the alkyl chain bands was measured with the facility available within spectral manipulation.

2.6. X-ray Photoelectron Spectroscopy (XPS) Measurements

The XPS spectra of quartz powder, albite powder and fractured surfaces, and both the surfaces treated with primary alkyl amines were recorded with AXIS Ultra (Kratos) electron spectrometer under Al monoirradiation and Mg irradiation with sample cooling. The vacuum in the sample analysis chamber during measurements was 10^{-8} Torr. A value of 285.0 eV was adopted as the standard C(1s) binding energy.

3.0. RESULTS AND DISCUSSION

3.1. Hallimond Flotation Studies

The flotation of quartz and albite as a function of C_8, C_{12} and C_{16} amine chlorides at pH 6–7 are shown in Fig. 1. The flotation responses with C_{12} and C_{16} amine acetate salts also presented in the same figure. The effect of alkyl chain length on the flotation behaviour of quartz (Fig. 1A) observed to be precisely the same as was presented by Fuerstenau *et al*. in 1964 [8]. The on-set of hemi-micelle formation for C_8, C_{12} and C_{16} amines corresponds to about 1×10^{-4}, 1×10^{-5} and 2×10^{-6} M respectively illustrating that the critical concentration decreases about one order magnitude with 4 carbons increase in the alkyl chain length. In the case of quartz, the counter ions of amine appear to have no influence since the flotation response is comparable with amine chloride and acetate solutions. However, the dodecylamine acetate salt gave higher flotation albite recovery than its chloride counter part (Fig. 1B), while the other conditions being the same. By outlining the fact that the flotation recovery is not sensitive with surface coverage of collector and one hydrophobic patch on the surface is enough for the particle to adhere air-bubble and float, the effect of acetate ion on amine adsorption cannot be ruled out.

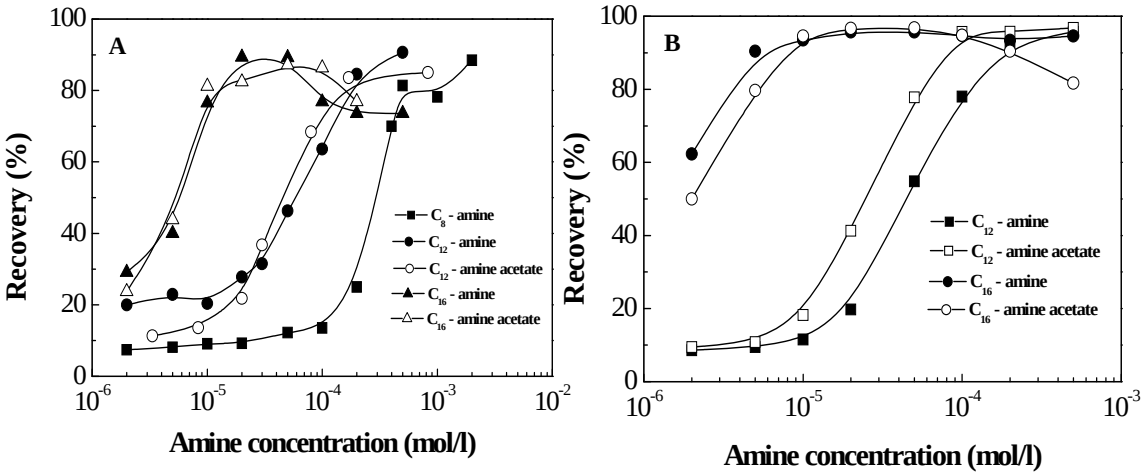

Fig. 1. Flotation of quartz (A) and albite (B) with amines as a function of concentration at pH 6–7.

3.2. Zeta-potential Studies

In Fig. 2, the zeta-potentials of quartz (Fig. 2A) and albite (Fig. 2B) under identical conditions to that of flotation studies (Fig. 1) are presented. For quartz, the hemi-micelle concentration for C_{12} amine is reached at about 4×10^{-4} M and for acetate salt, it corresponds to 7×10^{-4} M. These concentrations are more than one order magnitude higher when compared to flotation recovery curves. Similarly, the critical concentration for C_{16} amine where the zeta-potential raises towards positive is about 2×10^{-5} M in comparison to 1×10^{-6} M where the on-set of flotation is observed.

For C_8 amine, the zeta-potentials are either the same or increased the magnitude of negative charge until 2×10^{-3} M concentration distinguishing that the hemi-micelle concentration is not attained in the concentration range studied. Nevertheless, there is the on-set in flotation with C_8 amine at about 1×10^{-4} M (Fig. 1). For albite, the hemi-micelle concentration for C_{12} amine is reached about 1×10^{-4} M and for C_{16} amine is about 8×10^{-6} M. However, a good correlation between the adsorption of amine as evidenced from the area under the alkyl chain bands (3000–2800 cm^{-1}) and zeta-potentials is noticed (Fig. 2). The results show that there is a difference in the critical hemi-micelle concentration (CHC) in the zeta-potential and flotation curves. The difference could be due to the finer and coarser size particles used

respectively in these studies. The BET specific surface areas for quartz coarser and fine size fractions were determined to be 0.09 and 1.30 $m^2\ g^{-1}$ and the respective specific surface areas for albite size fractions were found to be 0.15 and 2.78 $m^2\ g^{-1}$. Considering the respective specific surface areas of the two size fractions for quartz and albite, the total surface area involved in either zeta-potential or flotation studies is approximately the same. The good correlation between flotation response, zeta-potential and adsorption density in C_{12} amine/quartz system reported by Fuerstenau [9], was from the zeta-potentials obtained by streaming potential measurements using coarser particles.

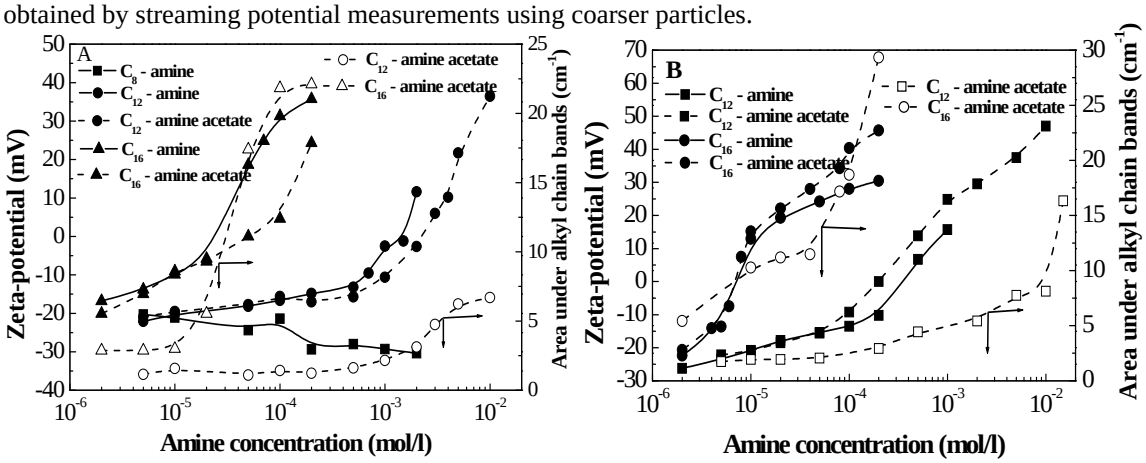

Fig. 2. Zeta-potentials of quartz (A) and albite (B) and adsorption of amine as a function of concentration at pH 6–7.

In the case of quartz, the onset amine concentration (CHC) of the steep increase in the zeta-potential curves with amines and their salts is varied with the acetate salt occurring at a slightly higher concentration. The co-adsorption of acetate ion would suppress the adsorption of amine so that the CHC for the ammonium acetate salt attains at a higher bulk amine concentration. The infrared studies presented later showed that acetate ions are adsorbed on quartz surface. The adsorption of acetate ions on a silicate surface through hydrogen and chemical bonding was reported [10].

3.3 Infrared Diffuse Reflectance Spectral Studies

The DRIFT spectra adsorption results of quartz and albite with C_{16} amines are presented in Fig. 3.

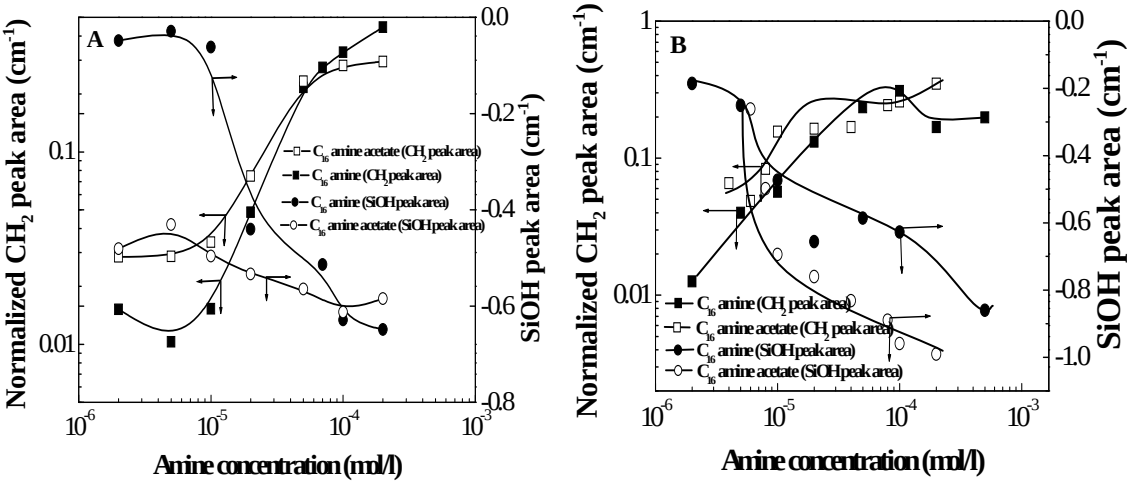

Fig. 3. Influence of C_{16} amine adsorption on quartz (A) and albite (B) silanol groups

Although the CH_2 peak area curves characterizing the adsorbed amine appear to be the same with increasing concentration until the break corresponding to the onset of CHC, the negative silanol groups area increases. This increase in negative area reached maximum at a certain bulk amine concentration. It signifies that the surface silanol groups are diminished because of the interaction with silanol groups. The bulk amine concentration until which the silanol groups are affected and the break in the adsorption curve, i.e., CHC, are found to be different in the case of amine and amine acetate. It suggests the influence of acetate counter ion on amine adsorption.

3.4. XPS Studies

Figure 4 shows the N(1s) spectra of the quartz powder treated with 4×10^{-5} and 2×10^{-4} M C_{12} amine acetate, and 2×10^{-4} M C_{12} amine. At amine concentration below CHC (curve 3), the spectrum is composed of one component at 400.1 eV. The spectra exhibit two components of N(1s) peak at CHC with binding energies of 399.5 eV and 401.5 eV. Similarly, the N(1s) spectrum of the albite conditioned in the 4×10^{-5} M solutions of C_{12} amine consists of a single peak at 401.4 eV and in the case of C_{12} amine acetate, a peak at 400.9 eV with a small satellite at 398.8 eV (Figure 5). While at a higher concentration (2×10^{-4} M) two N (1s) peaks 399.8 ± 0.1 and 401.2 ± 0.1 eV are present. These values, respectively, correspond to the binding energies of amino and ammonium groups when compared to the spectra of crystalline C_{12} amine and C_{12} amine acetate [11]. Thus, the adsorbed layer is composed of molecular alkyl amine and alkyl ammonium ions. The adsorption of amine on silanol groups can be realized with the amino group H-bonded to surface silanol attributed to the first component while the second component is attributed to the ammonium group formed owing to a charge transfer in strong H-bond between nitrogen of the amino and silanol groups [12-14]:

$$\equiv SiOH\ldots.H_2N\text{-}R \Leftrightarrow \equiv SiO^{-}\ldots H_3^{+}N\text{-}R \qquad (1)$$

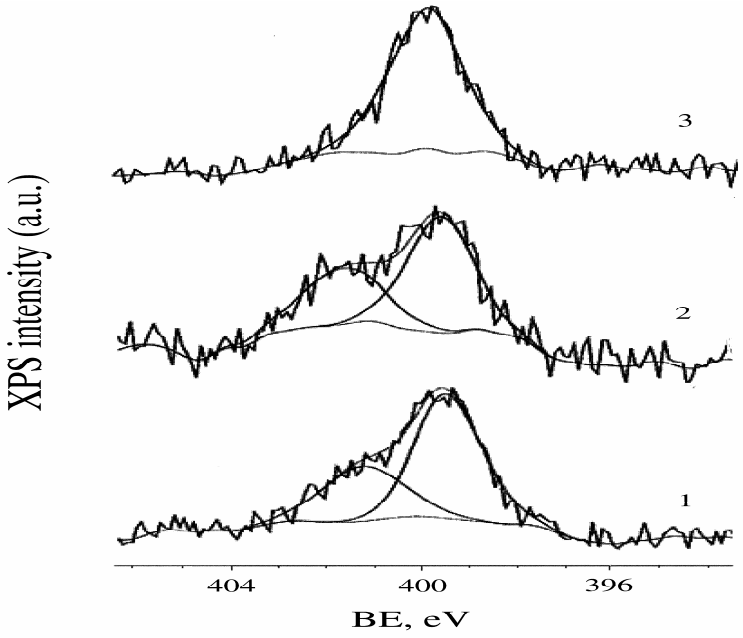

Fig. 4. XPS N(1s) spectra of quartz powder conditioned with (1) 2×10^{-4} M C_{12} amine; (2) 2×10^{-4} M C_{12} amine acetate; and (3) 4×10^{-5} M C_{12} amine acetate.

The above equilibrium exists at the interface once the molecular amine appears at the surface corresponding to CHC. The single peak for quartz and albite at concentrations less than CHC at 400.1 and 401.1 ± 0.3 eV respectively (Figs. 4 and 5) can thus be characterised by the ammonium group H-bonded to the silanols as:

$$\equiv Si - O \ldots H - {}^{+}NH_2 - R \qquad (2)$$

The NH…O bonds are weaker than the N…HO bonds and proton donating property of surface silanol groups is higher than its proton-accepting property in the H-bonding with a water molecule and acetic acid/acetate ion pair [15]. The transition from Eq (2) to Eq (1) is observed from infrared spectra where the broad band is centred at 3250 cm^{-1} at < CHC and shifting to 3000 cm^{-1} at > CHC. It is well known that a red shift of any H-bonded stretching mode points to the H-bond strengthening. Thus, the transition from Eq (2) to Eq (1) while strengthening H-bond occurring at CHC supports the above assignment of the N(1s) spectra.

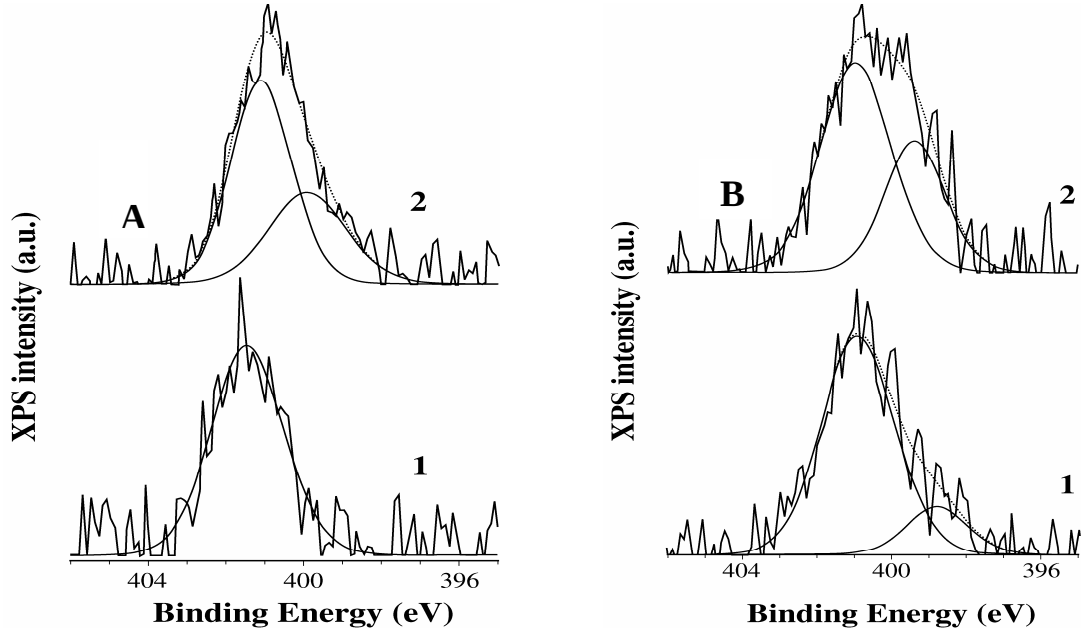

Fig. 5. XPS N(1s) spectra of a fracture albite surface conditioned in a solution (pH 6.5) of C_{12} amine acetate (A) and C_{12} amine (B). The amine concentrations are (1) 4×10^{-5} M; and (2) 2×10^{-4} M.

Thus, the extensively cited three regions of adsorption [6] can further be exemplified that i) An amine cation is H-bonded to surface silanol groups and this bond becomes stronger after the break in the adsorption characteristics (isotherm, zeta-potential, flotation); ii) at the break the origin of the adsorbed amine species changes qualitatively, and the molecular amine species appear together with an alkyl ammonium ion attached to deprotonated silanol group and thereby forming monolayer- thick patches of

well-oriented and densely packed adsorbed amine species, rendering the surface highly hydrophobic; and iii) at higher amine concentration, bulk precipitation of amine takes place.

4.0. ADSORPTION MECHANISM

The hemi-micelle model cannot explain the presence of neutral amine molecules in the adsorbed film below monolayer coverage and a strong H-bonding between amino head groups and the surface silanols. The present results can be interpreted within the framework of a two-dimensional condensation model if one substitutes the precipitation phenomena in place of condensation phenomena. However, before the transition to increased adsorption, the ammonium groups are hydrogen bonded to the negatively charged silanols (Eq (2)), and when the local concentration at the interface approaches a critical value, the adsorbed layer transforms into crystalline state owing to precipitation of neutral amine. At the first step, the process is two-dimensional and the adsorbed neutral amine establishes the equilibrium shown in Eq (1). Screening the electrostatic repulsion between head groups, the neutral molecules change the structure of the adsorbed layer substantially, increasing the density of the monolayer. The second phase transition of three-dimensional precipitation occurs when the bulk solubility limit is reached at the surface. This adsorption model is illustrated in Fig. 6 [11-14].

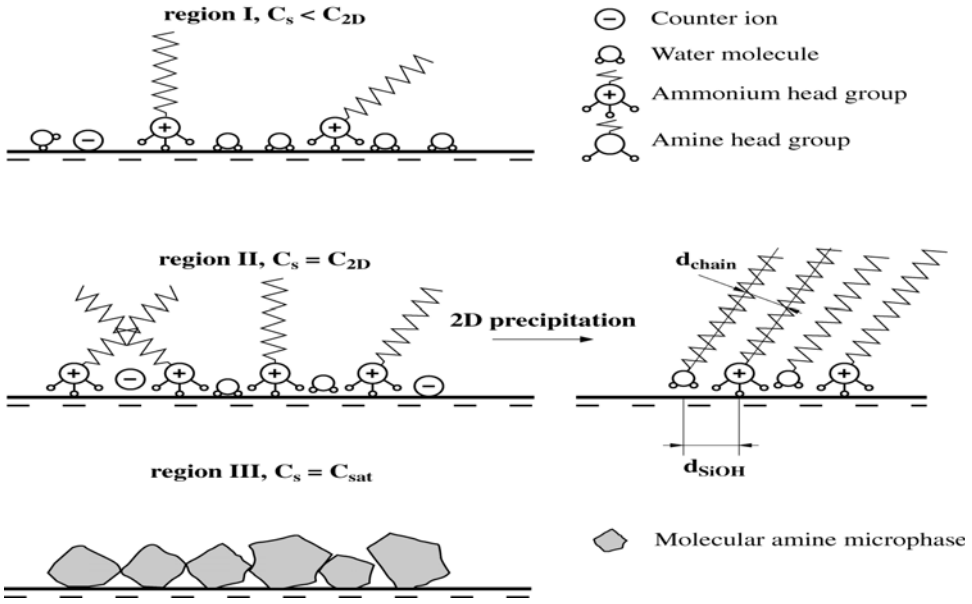

Fig. 6. Adsorption according to the 2D-3D precipitation mechanism

5.0 CONCLUSIONS

The adsorption mechanism of long-chain amines at neutral pH on quartz and albite has been studies using direct methods of FTIR and XPS spectroscopy and correlating the spectroscopic data with the data of the indirect methods zeta-potential and flotation tests. The infrared spectra showed that at low bulk amine concentrations, the surface silanol groups interact with ammonium groups through hydrogen bonds. After hemimicelle concentration, the XPS spectra showed neutral amine molecules along with the protonated ammonium ions coordinated to deprotonated silanol oxygen anions on the surface. Because of this adsorption steeply increases. At higher concentrations, the molecular amine precipitates on the surface. The later two regions of adsorption, where formation of neutral amines takes place, is affected by

the acetate counterions. However, the acetate counterions have no influence on flotation response. The results are interpreted in terms of successive two-dimensional and three-dimensional precipitation of amine on silicate surface.

6.0. REFERENCES

[1] J. Leja, *Surface Chemistry of Froth Flotation*, Plenum Press, New York, 1982.

[2] D.W. Fuerstenau, S. Raghavan: in: Proc.“ Int. Miner. Process. Congr”., Vol. II, D.N.P.M., Sao Paulo, 1980, pp. 368-415.

[3] R.W. Smith and J.L. Scott: *Miner. Process. Ext. Metall. Rev*. 1990, vol.7, pp. 81-94.

[4] J.S. Laskowski: in *Advances in Flotation Technology*, SME/AIME, Denver, Colorado, 1999 (eds. B.K. Parekh and J.D. Miller), pp. 59-82.

[5] A.M. Gaudin and D.W. Fuerstenau: *Trans. Soc. Min. Eng. AIME*. 1955, vol.202, pp. 958-962.

[6] P. Somasundaran and D.W. Fuerstenau: *J. Phys. Chem*. 1966, vol.79, pp. 90-97.

[7] D.W. Fuerstenau and H.M. Jang: Langmuir 1991, vol.7, pp. 3138.

[8] D.W. Fuerstenau, T.W. Healy and P. Somasundaran: *Trans. SME/AIME*. 1964, vol.229, pp. 321-325.

[9] D.W. Fuerstenau: *Min. Eng*. 1957, vol.208, pp. 1365-1367.

[10] J.D. Kubicki, L.M. Schroeter, M.J. Itih, B.N. Nguyen and S.E. Aptiz: *Geochim. Cosmochim. Acta*. 1999, vol.63, pp. 2709-2725.

[11] A. Vidyadhar, K. Hanumantha Rao, I.V. Chernyshova, Padip and K.S.E. Forssberg: J. Colloid Interface Sci.. 2002, vol.256, pp. 59-72.

[12] I.V. Chernyshova, K. Hanumantha Rao, A. Vidyadhar, and A. V. Shchukarev: *Langmuir* 2000, vol.16, pp. 8071-8084.

[13] I.V. Chernyshova, K. Hanumantha Rao, A. Vidyadhar and A. V. Shchukarev: *Langmuir* 2001, vol.17, pp. 775-785.

[14] A. Vidyadhar and K. Hanumantha Rao: J. Colloid Interface Sci.. 2007, vol.306, pp. 195-204.

[15] G.C. Pimentel and A.L. Mc Clellan: *The Hydrogen Bond*, Freeman, SanFrancisco, 1960.